Vertically aligned Si intrananowire p - n diodes by large-area epitaxial growth

Cheol-Joo Kim, Donghun Lee, Hyun-Seung Lee, Geunhee Lee, Gil-Sung Kim, and Moon-Ho Jo

Citation: Applied Physics Letters **94**, 173105 (2009); doi: 10.1063/1.3126037
View online: http://dx.doi.org/10.1063/1.3126037
View Table of Contents: http://scitation.aip.org/content/aip/journal/apl/94/17?ver=pdfcov
Published by the AIP Publishing

Vertically aligned Si intrananowire *p-n* diodes by large-area epitaxial growth

Cheol-Joo Kim,[1] Donghun Lee,[1] Hyun-Seung Lee,[1] Geunhee Lee,[1] Gil-Sung Kim,[1] and Moon-Ho Jo[1,2,a)]

[1]*Department of Materials Science and Engineering, Pohang University of Science and Technology (POSTECH), San 31, Hyoja-Dong, Nam Gu, Pohang, Gyungbuk 790-784, Republic of Korea*
[2]*Graduate Institute of Advanced Materials Science, Pohang University of Science and Technology (POSTECH), San 31, Hyoja-Dong, Nam Gu, Pohang, Gyungbuk 790-784, Republic of Korea*

(Received 27 October 2008; accepted 6 April 2009; published online 28 April 2009)

We demonstrate fabrication of vertically aligned, intrananowire *p-n* diodes by large-area epitaxial growth of Si nanowires (NWs). The axially modulated doping profile of *p-n* junctions is achieved by *in situ* doping with alternating addition of dopants in the axial sequence during Au-assisted chemical vapor deposition. We provide direct evidence of the intra-NW *p-n* junctions using scanning local probes in both individual NWs and vertically aligned NWs at large areas. Our study suggests implication for integrated electronics and optoelectronics based on bottom-up Si NWs. © *2009 American Institute of Physics*. [DOI: 10.1063/1.3126037]

Semiconductor *p-n* diodes are one of the basic circuit elements in various electronic, photonic, and photovoltaic devices, such as field-effect/bipolar junction transistors, photodiodes, and solar cells. Recently, various inter-/intrananowire (NW) *p-n* junctions based on the so-called bottom-up semiconductor NWs have been investigated by employing group IV, III-V, and II-VI semiconductor NWs for their unique optoelectronic properties at the nanometer scale.[1–5] Group IV semiconductor NWs are particularly interesting not only due to their wide recognition in microelectronics but also possible size effects in optical properties.[6–8] Here we report a controlled growth of vertically aligned,[9–12] intra-NW *p-n* diodes of Si NWs by large-area epitaxial growth. The axially modulated *p*- and *n*-dopant profiles within individual NWs are uniquely achieved by *in situ* doping during the Au-catalytic growth by high-vacuum chemical vapor deposition (CVD). We provide evidence that an individual Si NW possesses an intra-NW *p-n* diode by spatially resolved electrostatic force microscopy (EFM) and also confirm that the diode characteristics is maintained within the vertically aligned array at large areas.

Single-crystalline Si NWs were grown by Au catalyst-assisted CVD using 10% diluted SiH_4 precursors in H_2 in a quartz tube furnace.[8,13] We prepared Au catalysts by thermal evaporation of 2-nm-thick Au films on oxide-etched (111) Si substrates. Then the Au-coated Si substrates were immediately loaded into a quartz tube furnace, where the base pressure is pumped down to below 10^{-6} Torr. We carried out Au-catalytic NW growth at 690 °C under the SiH_4 partial pressure of 3.5 mTorr. In Fig. 1(a), a scanning electron microscopy (SEM) cross-sectional view shows the vertically aligned Si NWs with uniform lengths at a relatively large area. Transmission electron microscopy (TEM) images in Fig. 1(b) illustrate the initial growth stage of such vertical NWs by vapor-liquid-solid mechanism.[14,15] A high-resolution TEM image of the interface between the NW and a Si (111) substrate in the inset shows the NW grows along the [111] direction, and the continuous crystal planes across the interface without misfit dislocations or defects demonstrate the well-established epitaxy between the [111]-oriented NWs and Si (111) substrates. The top view SEM image in Fig. 1(c) shows that the growth directions of Si NWs are concentrated into four major orientations which correspond to the four equivalent ⟨111⟩ directions, as indicated by white arrows.[16] We find the typical occurrences of the orientations into the vertical ⟨111⟩ directions and the three nonvertical ⟨111⟩ directions are 75% and 25%, respectively. We note that the sidewalls of NWs in our growth are (112) faceted with hexagonal shapes in the NW radial directions and a periodic sawtooth shape along the NW axial direction, as in the inset. The same structural modulations have been attributed to the results of the interplay of geometry and surface energy of the wire and liquid droplet, when Au-catalytic NW growth occurs at high-vacuum CVD without the presence of background oxygen impurities.[17]

Having established the controlled growth of vertical NW arrays in an epitaxial manner, we further attempt to axially modulate the doping profile along the NWs by *in situ* doping

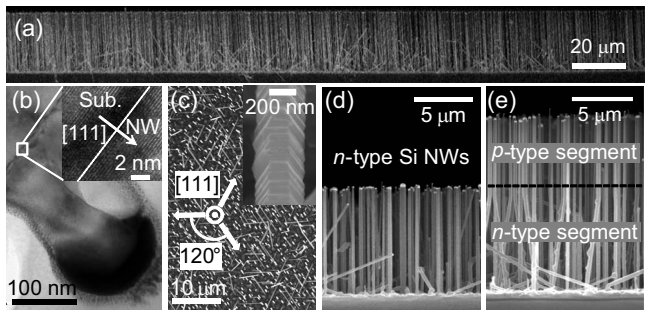

FIG. 1. (a) Cross-sectional view SEM image of vertically aligned Si NWs at large areas. (b) TEM image of an individual Si NW epitaxially grown on a Si (111) substrate. Inset is a high-resolution TEM image of the white box area. The interface between the NW and the substrate is indicated by a dotted line. (c) Top view SEM image of Si NWs grown on a Si (111) substrate. The inset shows that the sidewalls of NWs are (112) faceted with hexagonal shapes in the radial directions and periodic sawtooth shapes along the axial direction. (d) Cross-sectional view SEM image of P-doped Si NWs. (e) Cross-sectional view SEM image of Si intra-NW *p-n* diodes. The dotted line indicates the location of the *p-n* junctions.

a)Electronic mail: mhjo@postech.ac.kr.

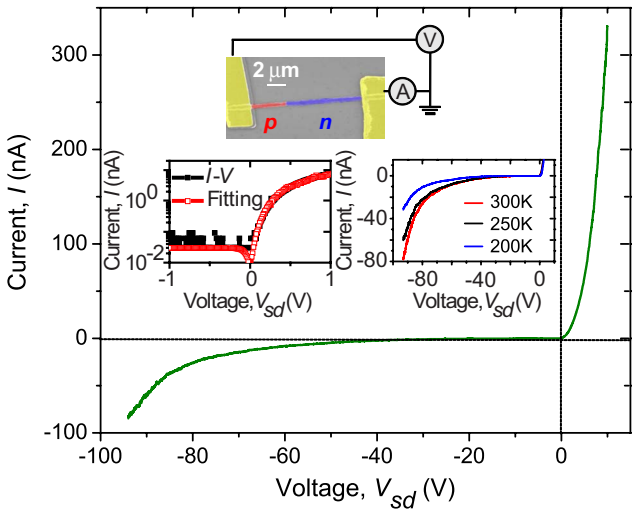

FIG. 2. (Color online) *I-V* characteristics of an individual Si NW *p-n* diode. The upper inset is the SEM image of the individual Si NW *p-n* diode. The lower left inset shows the *I-V* data at the low bias regime with a diode model fit. The lower right inset shows temperature-dependent *I-V* characteristics of the individual Si NW *p-n* diode.

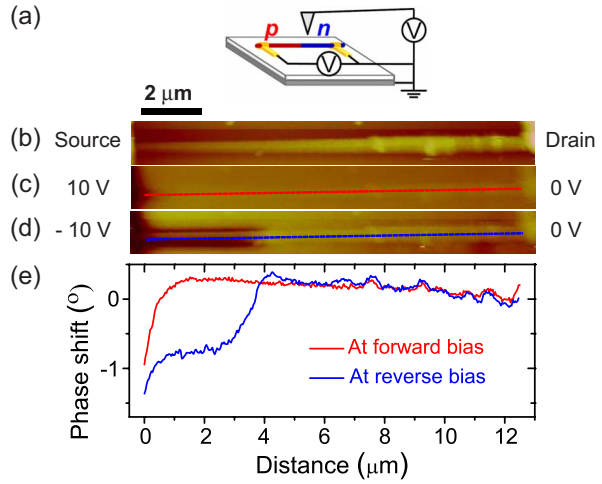

FIG. 3. (Color online) (a) EFM measurement setup. (b) AFM image of the individual Si NW *p-n* diode (c) EFM image at forward bias (10 V) applying at *p*-type region. (d) EFM image at reverse bias (−10 V) applying at *p*-type region. (e) EFM phase shift data along the dotted lines in the upper EFM images.

with alternating addition of PH_3 and B_2H_6 (100 ppm diluted in H_2) in the axial sequence during the SiH_4 catalytic growth. Nevertheless we found that the doping characteristics of the axially modulated NWs are governed by the latter dopants in the dopant feeding sequence, regardless of their types. We attribute this observation to the fact that a significant amount of the dopants may conformally incorporate into Si NWs through their surfaces as well as the catalytic decomposition in our growth conditions.[3,4] This observation is in contrast to an earlier report of Si NW *p-i-n* diodes by Yang *et al.*,[3] where the axial doping modulation has been achieved with the similar dopant precursors at a lower growth temperature. Our growth occurs at a relatively higher temperature under the lower base pressure of 10^{-6} Torr maintaining sufficiently clean Si NW surfaces, and this may lead to Au migration on Si NW surfaces during the growth.[18] This surface state can in turn activate conformal surface doping. It is known that *undoped* Si NWs grown by Au-catalytic growth using SiH_4 tend to exhibit *p*-type characteristics due to their surface states of hole accumulation, albeit they are relatively insulating.[19–21] Thus we attempt to achieve the axially modulated doping by the sequential growth of *n*-type segments in the presence of PH_3 in the first step, followed by the second growth step without the presence of PH_3, to form *p*-type segments (intrinsic segments). Figure 1(d) is a cross-sectional SEM image of P-doped Si NWs under the PH_3:SiH_4 ratio of $1:10^4$, and demonstrates that the vertical NW alignment is preserved upon *in situ* doping with a similar axial growth rate of 0.8–1.0 nm/s. We have observed that the NW shape tends to be tapered with random orientations when the PH_3:SiH_4 ratio exceeds over $3:10^4$.[22] The subsequent growth of intrinsic NWs without the presence of PH_3 maintains the vertical orientation, prolonged from the *n*-type seed NWs, as shown in Fig. 1(e).

Figure 2 shows the typical current-voltage (*I-V*) characteristics of an individual, modulation-doped Si NW device, as seen in the top inset of an SEM image.[23] It shows a typical current rectification with high current at forward bias >2–3 V and suppression at reverse bias down to <−80 V, suggesting the presence of the *p-n* junction within the NW channel. We also employed EFM scanning probes in order to spatially resolve electrical potential profiles along the individual NWs upon the current flowing at various bias voltages, as in Fig. 3. The contrast and the line profile in the EFM phase shift at the forward bias of 10 V, in Fig. 3(c), show that the major potential drop occurs at the contact between the source and the *p*-type segment that is more insulating than the *n*-type segment. By the separate two-probe resistivity measurements (thus including the contribution of contact resistance) of monolithic *p*-type (undoped) and *n*-type NWs (P-doped), we find the resistivity of 1.4×10^3 and 1.5×10^{-2} Ω cm, respectively. By sharp contrast, at the reverse bias of −10 V, the major potential drop occurs on the NW in addition to that at the contact, as seen in Figs. 3(d) and 3(e). This observation clearly illustrates that the current flowing is limited by the more insulating *p*-type NW segment in rectification, providing a large potential barrier within the NW. The *I-V* curve at the low bias regime is fitted with the diode model,

$$I = I_s\{\exp[e(V\text{-}R_sI)/nK_BT] - 1\}, \quad (1)$$

where I_s is the saturation current, R_s is the series resistance of NW, n is the ideality factor, K_B is Boltzmann's constant, and T is the temperature. The best fit is achieved with I_s =0.03 nA, n=2, R_s=90 MΩ, as shown in the lower left inset of Fig. 2. The ideal factor 2 usually suggests that thermal-generation current becomes dominant rather than diffusion current, and presumably in our diodes it can be attributed to the low intrinsic carrier density in an undoped *p*-type segment. Large series resistance may also be originated from the undoped *p*-type segment. It is notable that the breakdown voltage, where the reverse current rapidly increases, is marked at relatively large voltage (<−80 V), even after precluding the contribution of contact resistance to the total resistance. We can then estimate the breakdown field of the intra-NW *p-n* junction to be on the order of $\sim10^5$ V/cm, which is comparable to the breakdown field of intrinsic Si.[24] Particularly, as in the lower right inset of Fig. 2, we have found that the onset of the breakdown voltages negatively shifts with decreasing temperatures from all measured eight diodes. This negative temperature dependence of

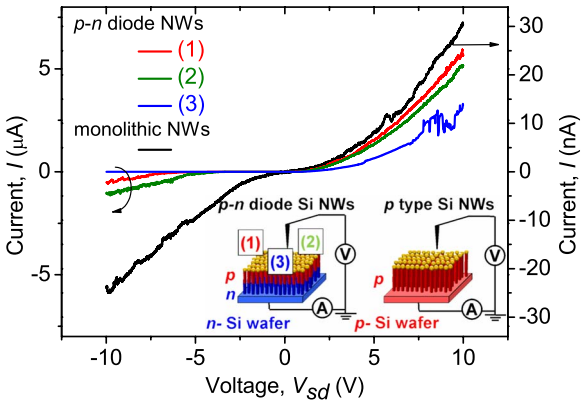

FIG. 4. (Color online) *I-V* characteristics of the vertically aligned, intra-NW *p-n* diodes and the monolithic *p*-type Si NW bundle, measured using cs-AFM tips. The low inset shows the schematic of the measurements. The relative size and the density of NWs are not scaled with respect to the tips for clarity.

the reverse-bias breakdown is in marked contrast to Si NW avalanche *p-i-n* photodiodes[2,3] synthesized by alternating *p-*/*n*-doping using gas-phase dopants, where the breakdown voltage shows the positive temperature dependence. The reverse junction breakdown is primarily associated with the doping profile and its resultant potential barrier within the junction. Our NW *p-n* diodes are different from the usual *p-i-n* NW diodes, in that they exploit surface-mediated *p*-type segments forgoing extrinsic *p*-type dopants of undoped segments, thus we speculate that this discrepancy can be attributed to the different surface state profiles along the junction. It should be also reminded that our NW sidewalls are in a periodic sawtooth shape, as mentioned above, and this also can affect the reverse junction leakage. This point is under further investigations by using other local probes, such as spatially resolved photocurrent measurements.

Finally we have further investigated *I-V* characteristics of the array NW *p-n* diodes using a current sensing atomic force microscopy (cs-AFM), as seen in the inset of Fig. 4. Here the vertical *p-n* diode NWs were grown on heavily *n*-type doped Si substrates, and the electrical contact to the top of NWs has been made using a PtIr5 coated tip. In order to ensure the reproducible electrical contacts between NWs and the cs-AFM tip, we lowered the scanning tip down below the top of NW arrays until the observed current was stably saturated. At various positions within the NW arrays, the *I-V* characteristics are consistently rectifying with a similar forward bias current. Typically we observed the forward bias current at 10 V of ~5 μA. By a simple comparison with Fig. 3, this current amplitude can be regarded as a sum current contributed from about 25 NWs without considering inhomogeneous contacts between constituent NWs and the local tip electrodes. As a reference, we also prepared undoped NW arrays grown on heavily *p*-type doped Si substrates by the same manner, as indicated in the right inset. As shown in Fig. 4, the current of the undoped NWs is symmetric for forward and reverse bias, and its amplitude is also suppressed by two orders of magnitude. This direct comparison demonstrates that fabrications of intrananowire *p-n* diodes arrays can be available by large-area epitaxial growth based on the controlled growth.

This work was supported by Nano R&D program through the KOSEF (Grant No. 2007-02864), the 2008 MEST-AFOSR NBIT, the KRF Grant MOEHRD (Grant No. KRF-2005-005-J13103), SRC/ERC program of MEST/KOSEF (Grant No. R11-2008-105-01003-0) and through the WCU program by MEST (Grant No. R31-2008-000-10059-0).

[1]M. S. Gudiksen, L. J. Lauhon, J. Wang, D. C. Smith, and C. M. Lieber, Nature (London) **415**, 617 (2002).
[2]O. Hayden, R. Agarwal, and C. M. Lieber, Nature Mater. **5**, 352 (2006).
[3]C. Yang, C. J. Barrelet, F. Capasso, and C. M. Lieber, Nano Lett. **6**, 2929 (2006).
[4]E. Tutuc, J. Appenzeller, M. C. Reuter, and S. Guha, Nano Lett. **6**, 2070 (2006).
[5]B. Tian, X. Zheng, T. J. Kempa, Y. Fang, N. Yu, G. Yu, J. Huang, and C. M. Lieber, Nature (London) **449**, 885 (2007).
[6]H. Takagi, H. Ogawa, Y. Yamazaki, A. Ishizaki, and T. Nakagiri, Appl. Phys. Lett. **56**, 2379 (1990).
[7]S. Schuppler, S. L. Friedman, M. A. Marcus, D. L. Adler, Y.-H. Xie, F. M. Ross, T. D. Harris, W. L. Brown, Y. J. Chabal, L. E. Brus, and P. H. Citrin, Phys. Rev. Lett. **72**, 2648 (1994); T. van Buuren, L. N. Dinh, L. L. Chase, W. J. Siekhaus, and L. J. Terminello, *ibid.* **80**, 3803 (1998).
[8]J.-E. Yang, C.-B. Jin, C.-J. Kim, and M.-H. Jo, Nano Lett. **6**, 2679 (2006).
[9]A. I. Hochbaum, R. Fan, R. He, and P. Yang, Nano Lett. **5**, 457 (2005).
[10]Y. Wang, V. Schmidt, S. Senz, and U. Gösele, Nat. Nanotechnol. **1**, 186 (2006).
[11]S. Ge, K. Jiang, X. Lu, Y. Chen, R. Wang, and S. Fan, Adv. Mater. (Weinheim, Ger.) **17**, 56 (2005).
[12]K. Q. Peng, Z. P. Huang, and J. Zhu, Adv. Mater. (Weinheim, Ger.) **16**, 73 (2004).
[13]C.-B. Jin, J.-E. Yang, and M.-H. Jo, Appl. Phys. Lett. **88**, 193105 (2006).
[14]R. S. Wagner and W. C. Ellis, Appl. Phys. Lett. **4**, 89 (1964).
[15]A. M. Morales and C. M. Lieber, Science **279**, 208 (1998).
[16]V. Schmidt, S. Senz, and U. Gösele, Nano Lett. **5**, 931 (2005).
[17]F. M. Ross, J. Tersoff, and M. C. Reuter, Phys. Rev. Lett. **95**, 146104 (2005).
[18]S. Kodambaka, J. B. Hannon, R. M. Tromp, and F. M. Ross, Nano Lett. **6**, 1292 (2006).
[19]Y. Cui, X. Duan, J. Hu, and C. M. Lieber, J. Phys. Chem. B **104**, 5213 (2000).
[20]Y. Wang, K.-K. Lew, T.-T. Ho, L. Pan, S. W. Novak, E. C. Dickey, J. M. Redwing, and T. S. Mayer, Nano Lett. **5**, 2139 (2005).
[21]Y. H. Ahn and J. Park, Appl. Phys. Lett. **91**, 162102 (2007).
[22]H. Schmid, M. T. Bjork, J. Knoch, S. Karg, H. Riel, and W. Riess, Nano Lett. **9**, 173 (2009).
[23]C.-J. Kim, W.-H. Park, J.-E. Yang, H.-S. Lee, S. Maeng, Z. H. Kim, H. M. Jang, and Moon-Ho Jo, Appl. Phys. Lett. **91**, 033104 (2007).
[24]S. M. Sze, *Physics of Semiconductor Devices*, 2nd ed. (Wiley, New York, 1981), Vol. 2, p. 84.